Electroreduction of Oxygen in Polymer Electrolyte Fuel Cells by Activated Carbon Coated Cobalt Nanocrystallites Produced by Electric Arc Discharge

G. Lalande, D. Guay, and J. P. Dodelet*

INRS-Énergie et Matériaux, C.P. 1020, Varennes, Québec, Canada, J3X 1S2

S. A. Majetich† and M. E. McHenry‡

Departments of Physics and Materials Science and Engineering, Carnegie Mellon University, Pittsburgh, Pennsylvania 15213-3890

Received September 16, 1996. Revised Manuscript Received November 6, 1996⊗

Carbon-coated fcc cobalt nanocrystallites produced by the carbon arc method have practically no activity as catalysts for O_2 reduction in H_2/O_2 polymer electrolyte fuel cells. This material, containing 17.0 wt % Co, was activated by a pyrolysis step at 1000 °C in Ar containing acetonitrile vapor. When it was used at the cathode of a single fuel cell element, it provided an initial current of 0.10 A/cm^2 mg of Co at 0.5 V and 50 °C. This current decreased by 40% after 300 h. Only a fraction of the carbon-coated metal in the initial material was activated by the pyrolysis treatment. XPS and TEM characterizations were performed on the catalyst at various stages of its preparation.

Introduction

Polymer electrolyte fuel cells (PEFCs) are efficient, nonpolluting, low-noise electrical generators. They have been developed mainly for transportation, but stationary applications are now also considered.[1−4] These generators produce electrical power from two electrochemical reactions: H_2 oxidation at the anode and O_2 reduction at the cathode. The electrical circuit is completed by the diffusion of protons through the polymeric membrane which has a pH of about 1 when humidified.[5] Catalysts are used to increase the reaction rate of both electrochemical reactions. All commercial PEFC prototypes use Pt or Pt alloys as catalysts for both reactions. However, Pt is an expensive metal of limited supply. Its utilization in PEFCs is one of the reasons these electrical generators are not widely used despite their multiple energetic and environmental advantages.

In the field of PEFCs, research on catalysts is centered on either reducing the Pt loading or replacing it by a nonnoble metal. Experiments have been carried out during the last several years to replace Pt at the cathode by catalysts based on organometallic compounds adsorbed on carbon black and pyrolyzed at various temperatures.[6−9] We have also worked on pyrolyzed Co and Fe phthalocyanines and porphyrins for O_2 reduction.[10−15] It was found that catalysts that are at the same time efficient and relatively stable are obtained by the pyrolysis of the organometallic precursors at high temperature (≥800 °C).

It is important in electrocatalysis to identify the catalytic site. In our previous work on Co and Fe organometallic compounds adsorbed on carbon black and pyrolyzed at temperatures higher than 800 °C, we have always observed Co and Fe metallic particles surrounded by a carbon coating. High-resolution TEM on Co-based catalysts even showed that this coating displayed a graphitic structure.[16] We assumed therefore that these carbon-coated metal clusters were the catalytic sites for oxygen reduction in these materials. However, in an attempt to determine what elements are necessary to produce the catalytic sites, we recently used another precursor, polyvinylferrocene (PVF), which is a molecule made of C and Fe only.[17] PVF was adsorbed on carbon black (PVF/C) and pyrolyzed at 1000 °C in various ambients. The main observations made about the catalytic properties of pyrolyzed PVF/C were as follows:

* To whom correspondence should be addressed.
† Department of Physics.
‡ Department of Materials Science and Engineering.
⊗ Abstract published in *Advance ACS Abstracts,* February 1, 1997.

(1) Appleby, A. J. *Int. J. Hydrogen Energy* **1994**, *19*, 175.
(2) Prater, K. B. *J. Power Sources* **1994**, *51*, 129.
(3) Barbir, F. *NATO ASI Ser., Ser. E* **1995**, *295 (Hydrogen Energy System)*, 241.
(4) Prater, K. B. SPFC Fuel Cells for Transport and Stationary Applications. Fourth Grove Fuel Cell Symposium, London, 1995; Book of Abstracts.
(5) Appleby, A. J. *J. Electroanal. Chem*. **1993**, *357*, 117.
(6) Wiesener, K. *Electrochim. Acta* **1986**, *31*, 1073.
(7) Wiesener, K.; Ohms, D.; Neumann, V.; Franke, R. *Mater. Chem. Phys.* **1989**, *22*, 457.
(8) Tarasevich, M. R.; Radyushkina, K. A. *Mater. Chem. Phys.* **1989**, *22*, 477.
(9) Vasudevan, P.; Santosh; Mann, N.; Tyagi, S. *Transition Met. Chem*. **1990**, *15*, 81.
(10) Martin Alves, M. C.; Dodelet, J. P.; Guay, D.; Ladouceur, M.; Tourillon, G. *J. Phys. Chem*. **1992**, *96*, 10898.
(11) Ladouceur, M.; Lalande, G.; Guay, D.; Dodelet, J. P.; Dignard-Bailey, L.; Trudeau, M. L.; Schulz, R. *J. Electrochem. Soc.* **1993**, *140*, 1974.
(12) Tamizhmani, G.; Dodelet, J. P.; Guay, D.; Lalande, G.; Capuano, G. *J. Electrochem. Soc.* **1994**, *141*, 41.
(13) Lalande, G.; Tamizhmani, G.; Côté, R.; Dignard-Bailey, L.; Trudeau, M. L.; Schulz, R.; Guay, D.; Dodelet, J. P. *J. Electrochem. Soc.* **1995**, *142*, 1162.
(14) Faubert, G.; Lalande, G.; Côté, R.; Guay, D.; Dodelet, J. P.; Weng, L. T.; Bertrand, P; Denès, G. *Electrochim. Acta* **1996**, *41*, 1689.
(15) Lalande, G.; Faubert, G.; Côté, R.; Guay, D.; Dodelet, J. P.; Weng, L. T.; Bertrand, P. *J. Power Sources*, in press.
(16) Dignard-Bailey, L.; Trudeau, M. L.; Joly, A.: Schulz, R.; Lalande, G.; Guay, D.; Dodelet, J. P. *J. Mater. Res.* **1994**, *9*, 3203.
(17) Lalande, G.; Côté, R.; Guay, G.; Dodelet, J. P.; Weng, L. T.; Bertrand, P. *Electrochim. Acta*, in press.

S0897-4756(96)00479-6 CCC: $14.00 © 1997 American Chemical Society

1. *The pyrolysis of PVF/C in Ar* produces a material exhibiting no catalytic activity. Transmission electron microscopy (TEM) and X-ray diffraction (XRD) analysis revealed the presence of carbon-coated Fe nanoparticles in the material with the carbon coating protecting the Fe particles from dissolving in an acidic medium. This observation indicates therefore that the carbon-coated metal particles detected previously by TEM are probably not associated with the catalytic sites.

2. A material displaying catalytic activity for O_2 reduction is obtained when PVF/C is *pyrolyzed in Ar containing acetonitrile (CH_3CN) vapor*. Acetonitrile (AN) is thermally decomposed in the reactor, thus providing the nitrogen necessary to the generation of the catalytic site. Contrary to the previous case, TEM analysis of this material did not reveal any carbon-coated metal particles. This new method of producing catalysts has been generalized by replacing PVF by $Fe(OH)_2$. A catalyst for O_2 reduction is obtained when $Fe(OH)_2$/C is pyrolyzed at 1000 °C in Ar containing AN vapors.[18] Nanotubes containing metal particles are observed by TEM in the active material.

3. The catalytically inactive carbon-coated Fe nanoparticles obtained by the pyrolysis of PVF/C in Ar can be activated by a second pyrolysis step performed in Ar containing AN vapor. TEM analysis of the new material indicated a decrease in the number of carbon-coated Fe clusters compared to that found after the first pyrolysis in Ar. Nanotubes containing metal particles were also observed.

At this point in our research on the nature of the catalytic site for oxygen reduction in high-temperature pyrolyzed materials, it is important to confirm and maybe generalize our findings with PVF/C by showing (i) that carbon-coated metal particles obtained by a method completely different from our usual pyrolysis procedure are also inactive materials and (ii) that it is also possible to activate them by the same high-temperature treatment in acetonitrile vapors. To do so, we used *Co particles produced by carbon arc discharge* as starting material. The Kratschmer carbon arc is indeed a versatile system that was first used to obtain macroscopic amounts of fullerenes[19] and macroscopic quantities of nanotubes.[20] Following the arc synthesis of fullerenes and nanotube structures, it was reported that single-domain microcrystals of LaC_2 encapsulated with nanoscale polyhedral carbon particles were also synthesized in a carbon arc.[21] Then, nanometric Fe_3C particles[22] and Co clusters[23] coated with a few graphite layers were also reported, together with the generation in the carbon arc reactor of single-shell carbon nanotubes. A recent review of the encapsulation of rare earth and iron group metals (Fe, Co, Ni) using electric arc discharge has been published by Saito.[24]

In the present work, it will be shown that the carbon-coated Co nanocrystallites obtained by the Kratschmer carbon arc process are indeed catalytically inactive materials for O_2 reduction. These materials can however be activated by pyrolysis at 1000 °C in AN vapors. This activation procedure seems therefore to be quite general since it can turn either hydroxides adsorbed on carbon black[18] or any inactive carbon-coated metal into catalysts for O_2 reduction. It will however be shown that these catalysts are not equivalent when their performances are compared.

Experimental Section

Catalyst Synthesis. The carbon-coated fcc cobalt nanocrystallites were prepared by a process based on the Kratschmer−Huffman carbon arc method from a mixture of Co_3O_4, graphite powder, and graphite cement. Details about the experimental procedure and the characterization of the nanocrystallites are reported in ref 25.

A catalyst for O_2 reduction was obtained by activation of this material. A fused silica boat containing 0.3 g of the carbon-coated Co powder was introduced in a fused silica tube, which was purged during 30 min with Ar bubbling in acetonitrile (CH_3CN) maintained at room temperature. The tube was then placed in a split furnace preheated at 1000 °C and left at that temperature for 2 h. Then, the tube was removed from the furnace and allowed to cool to room temperature before stopping the gas flow.

Bulk and Surface Characterizations. Bulk Co concentrations were obtained from neutron activation analysis performed at l'École Polytechnique de Montréal. Transmission electron microscopy (TEM) was performed on a JEOL 2000FX microscope operating at 200 kV or a Philips CM-30 microscope operated at 300 kV. Specimen preparation consisted of dispersing the materials in 2-propanol using an ultrasonic bath. A drop of the dispersion was deposited on the TEM carbon-coated copper grid and left to dry. Surface analyses were performed by X-ray photoelectron spectroscopy (XPS) on a VG ESCALAB200i. The monochromated Al Kα line at 1486.6 eV was used. The powder samples were fixed on an adhesive Cu tape. No charging problems were encountered. Narrow scan photoelectron spectra were recorded for the C1s, N1s, $Co2p_{3/2}$, and O1s core levels. A semiquantitative analysis of the XPS data was performed according to the procedure described in ref 26.

Electrochemical Measurements. The catalysts were evaluated electrochemically in half and full cells. Measurements in half cells were obtained by the rotating disk electrode technique (RDE). The experimental setup and procedure are described in detail elsewhere.[12,26] The electrolyte was H_2SO_4 at pH 0.5, saturated with O_2. Cyclic voltammograms were recorded at room temperature between 0 and 0.7 V vs SCE (unless otherwise specified) at a scan rate of 10 mV/s and rotational speeds of 0 and 1500 rpm. The catalytic activity for O_2 reduction was qualitatively evaluated by determining the potential at maximum reduction current in the voltammogram recorded at 0 rpm.

Measurements in full cells were obtained with 5 cm^2 gas diffusion electrodes (GDE) and a Nafion 117 membrane in a fuel cell test station (Globe-Tech). The anode consisted of an uncatalyzed ELAT carbon backing structure (from E-TEK), catalyzed with 0.37 mg/cm^2 (20 wt %) Pt. The anode was painted with two layers of a 5 wt % Nafion solution, then dried at 75 °C for 2 h under vacuum. The dry Nafion loading was about 0.6 mg/cm^2. The cathode was prepared as follows: a mixture containing 27.5 mg of catalyst, 0.6 mL of deionized water, and 0.6 mL of 5 wt % Nafion solution was blended ultrasonically in a closed vial for 30 min; 0.55 mL of the paint was pipetted and spread on an uncatalyzed ELAT backing;

(18) Fournier, J.; Lalande, G.; Côté, R.; Guay, D.; Dodelet, J. P. *J. Electrochem. Soc.*, in press.
(19) Kratschmer, W.; Lamb, L. D.; Fostiropoulos, K.; Huffman, D. R. *Nature* **1990**, *347*, 354.
(20) Ebbesen, T. W.; Ajayan, P. M. *Nature* **1992**, *358*, 220.
(21) Ruoff, R. S.; Lorentz, D. C.; Chan, B.; Malhotra, R.; Subramoney, S. *Science* **1993**, *259*, 346.
(22) Iijima, S; Ishihashi, J. *Nature* **1993**, *363*, 603.
(23) Bethune, D. S.; Kiang, C. H.; de Vries, M. S.; Gorman, G.; Savoy, R.; Vazquez, J.; Beyers, R. *Nature* **1993**, *363*, 605.
(24) Saito, Y. *Carbon* **1995**, *33*, 979.
(25) McHenry, M. E.; Majetich, S. A.; Artman, J. O.; De Graef, M.; Staley, S. W. *Phys. Rev. B* **1994**, *49*, 11358.
(26) Lalande, G.; Côté, R.; Tamizhmani, G.; Guay, G.; Dodelet, J. P.; Dignard-Bailey, L.; Weng, L. T.; Bertrand, P. *Electrochim. Acta* **1995**, *40*, 2635.

the paint was allowed to dry; a second similar coating was applied on the cathode which was then dried at 75 °C for 2 h under vacuum. The Co metal loading in these cathodes was about 0.28 mg/cm^2. The cathode using 2 wt % Pt from ETEK contained 0.17 mgof Pt/cm^2. It was prepared by the successive deposition on the cathode of four 60 μL layers of solution composed of 17.1 mg of catalyst, 0.24 mL of a 5 wt % Nafion solution, and 0.24 mL of deionized water. A single-cell assembly was prepared by pressing the anode, membrane, and cathode at 140 °C for 40 s and under 2500 pounds of pressure. The polarization and stability tests were performed at a cell temperature of 50 °C. H_2/O_2 gas pressures were 30/60 psi, and their flow rates are both 0.1 L/min. Both gases were humidified in stainless steel containers filled with deionized water kept at 75 °C before being admitted into the single-cell fixture. Before running polarization and stability tests, the cell was left 1 h under open-circuit conditions. The stability test was run during 300 h at 0.5 V vs RHE immediately after measuring the polarization curve.

Results and Discussion

The Materials: CCo, wCCo, CCo + AN, wCCo + AN. Four kinds of materials were analyzed. They all derive from the carbon-coated nanocrystalline metal obtained by the carbon arc method (CCo). This material contains 17.0 wt % of Co. RDE experiments indicates that part of the material oxidizes during the first voltammetric cycle between 0 and 0.7 V vs SCE. An XPS survey spectrum shows the presence of Zn (2.8 at. % or 12.6 wt %) in CCo. This element is a surface contaminant (originating probably from brass rod holders in the reactor) because its surface concentration determined by XPS (12.6 wt %) is practically identical with its bulk concentration determined by neutron activation analysis (13.1 wt %). The accuracy of metal dosimetry by XPS is ±10 wt %, while it is ±5 wt % for neutron activation analysis. Zn is completely removed by washing CCo for 4 h in warm formic acid. This material is labeled wCCo. Neutron activation analysis indicates that wCCo contains 17.7 wt % Co and <0.4 wt % Zn. Therefore, all Zn (but only little Co) is lost during the washing process. This is a further proof that the initial Zn content is not representative of the nanoparticles. The Co wt % increase in wCCo compared to CCo is attributable to the loss of Zn. The other two materials studied in this work are the catalysts which are obtained by activating CCo and wCCo at 1000 °C in Ar + acetonitrile (AN). They are labeled CCo + AN and wCCo + AN, respectively.

Electrochemical Results. Figure 1 presents the cyclic voltammograms obtained at 0 and 1500 rpm for three materials: (A) CCo; (B) CCo + AN; (C) wCCo + AN. The voltammogram obtained for wCCo is the same as that of CCo (Figure 1A). At 0 rpm, the potential at maximum cathodic current peak is 0.025 V for CCo or wCCo (A), 0.265V for CCo + AN (B), and 0.215V for wCCo + AN (C). Upon rotation, the current associated with the peak at 0 rpm increases, confirming that it is related to O_2 reduction. It is clear from those experiments that (i) heat treatment in Ar containing AN vapor is effective in generating active catalysts for O_2 reduction from rather inactive materials and (ii) that CCo + AN is a better catalyst than wCCo+AN.

A similar conclusion is reached from the GDE polarization curves presented in Figure 2 for a single element of a H_2/O_2 fuel cell made with cathodes containing either CCo + AN or wCCo + AN. Fuel cell tests were not performed on CCo or wCCo because these materials showed practically no catalytic activity for O_2 reduction in the RDE experiments.

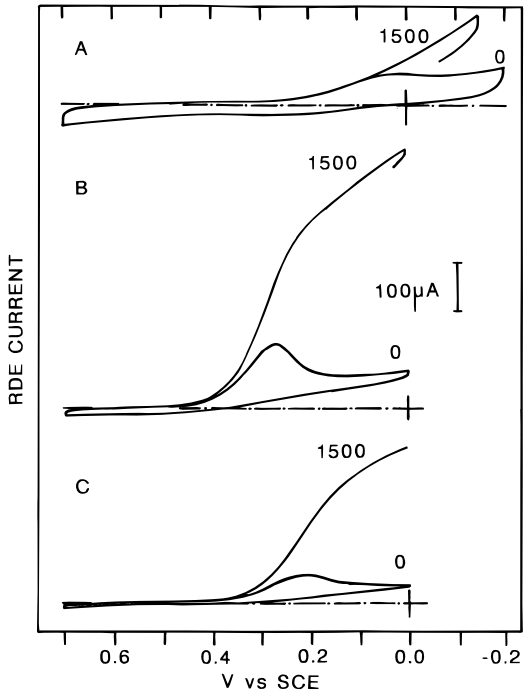

Figure 1. 1. Cyclic voltammograms obtained at 0 and 1500 rpm for (A) CCo, (B) CCo + AN, and (C) wCCo + AN.

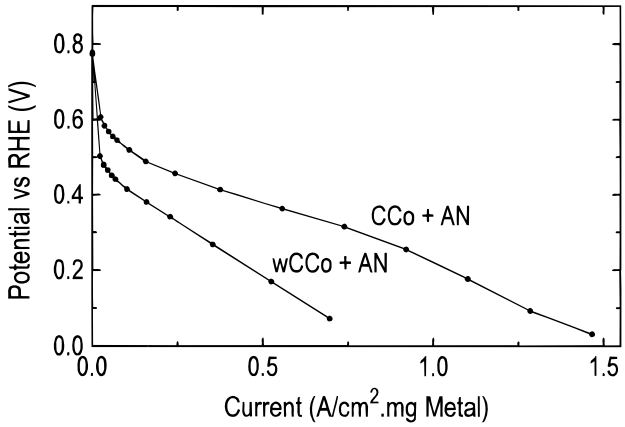

Figure 2. 2. Polarization curves recorded at 50 °C in a single element of a H_2/O_2 fuel cell using CCo + AN or wCCo + AN as cathode catalysts.

Figure 3 presents fuel cell stability tests at 0.5V vs RHE and 50 °C for CCo + AN and wCCo + AN. The current vs time curves were obtained after recording the polarization curves shown in Figure 2. As seen from Figure 3, both catalysts lack stability and lose 40−55% of their initial activity after 300 h of operation. This may be due to a slow dissolution of some Co nanoparticles that are not completely protected from the corrosive acidic medium. Stable activity has only been recently achieved with a catalyst made of polyvinylferrocene (PVF) adsorbed on carbon black and pyrolyzed at 1000 °C in Ar + AN. In that case, a current of 0.6 A/cm^2 mg of Fe was sustained for 300 h in a fuel cell at 0.5 V and 50 °C.[17] For comparison, in the same conditions, a 2 wt % Pt commercial catalyst from ETEK gives 1.8 A/cm^2 mg of Pt.

It is obvious from these comparisons that the catalysts produced in this work are moderately active since the

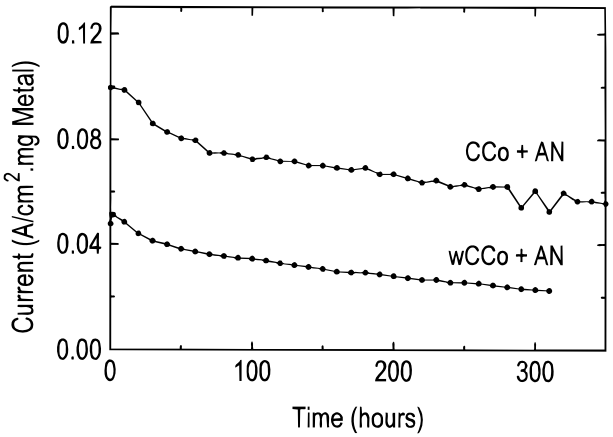

Figure 3. 3. Stability tests performed at 50 °C in a single element of a H_2/O_2 fuel cell using CCo + AN or wCCo + AN as cathode catalysts.

Table 1. XPS Surface Concentrations in Atomic Percent (at. %) and in Weight Percent (wt %) of the Catalysts and Their Precursors

	CCo	wCCo	CCo + AN	wCCo + AN
C (at. %)	83.3	89.4	89.4	90.4
Co (at. %)	1.7	1.2	0.5	0.4
N (at. %)	0.8	0.7	7.5	6.9
O (at. %)	11.4	8.7	2.6	2.3
Zn (at. %)	2.8	0.0	0.0	0.0
Co (wt %)	6.8	5.3		
O (wt %)	12.4	10.7		
Zn (wt %)	12.6	0		

highest current (0.1 A/cm^2 mg of metal) obtained from the best material (CCo + AN) at 0.5 V and 50 °C is only 5% of what is obtained from a 2 wt % Pt catalyst. This may be partly explained by the fact that only a fraction of the carbon-coated Co metal particles in CCo or wCCo is activated by the pyrolysis treatment at 1000 °C in Ar + AN. Furthermore, no conductive carbon black support is used with CCo + AN.

XPS and XRD Results. Table 1 reports the surface concentrations of the major elements detected in CCo and wCCo before and after their activation with AN. Figures 4 and 5 present the XPS narrow scan spectra of the Co2$p_{3/2}$ and N1s core levels of CCo, wCCo, and wCCo + AN, respectively. Considering the XPS results, the following observations can be made:

1. The Co surface concentrations in CCo and wCCo are 6.8 and 5.3 wt %, respectively, while the corresponding bulk concentrations are 17.0 and 17.7 wt %. This important difference between the bulk and surface concentrations results from the fact that several Co clusters in CCo and wCCo are larger than the escape depth of the photoelectrons in these materials (about 3 nm). Co photoelectrons could also remain trapped in the materials if the carbon coatings are too thick. Both hypotheses will be confirmed by TEM.

2. Co in CCo is detected as metallic Co (the peak at 778.5 eV in Figure 4 [27]) and as an oxide (the shoulder at higher binding energy[28]). The oxidized form of Co is absent from the Co2$p_{3/2}$ narrow-scan spectrum of wCCo. Cobalt oxide has therefore been removed from CCo by acid washing. This observation indicates that

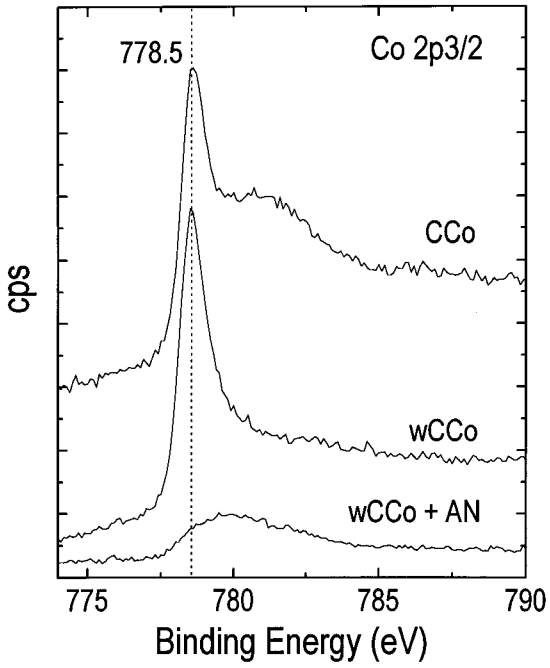

Figure 4. 4. XPS narrow scan spectra of the Co2$p_{3/2}$ core level of CCo, wCCo, and wCCo + AN.

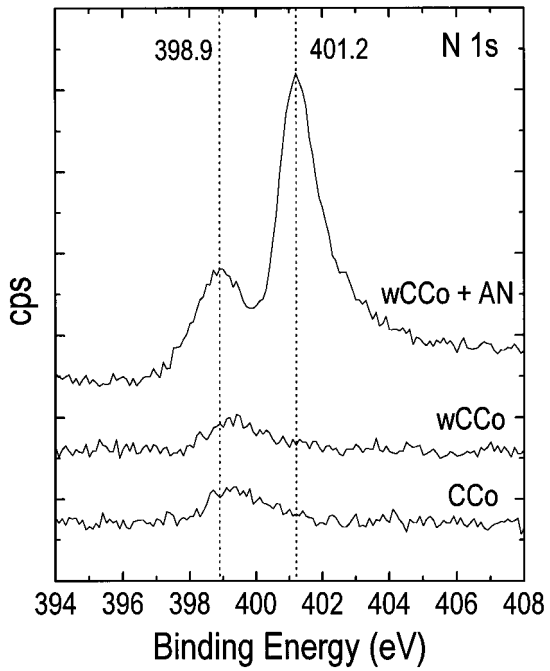

Figure 5. 5. XPS narrow scan spectra of the N1s core level of CCo, wCCo, and wCCo + AN.

cobalt oxide was not carbon-coated. The amount of Co lost during acid washing represents only a small fraction of the initial bulk concentration. A maximum of 2.3 wt % Co is lost if it is assumed that surface and bulk weight contents of oxygen are equal. Metallic Co has also been detected by X-ray diffraction analysis of CCo. The pattern reported in ref 25 indicates the presence of the fcc cobalt phase along with the predominant graphitic peaks and a broadened peak at small angles characteristic of the fullerenes. No evidence was found by XRD analysis for the presence of oxides or the metastable carbides. The oxide signal detected by XPS is therefore mainly generated by a thin oxide layer at the surface of a small fraction (2.3 wt %) of the Co crystallites that

(27) Choudhury, T.; Saied, S. O.; Sullivan, J. L.; Abbot, A. M. *J. Phys. D, Appl. Phys.* **1989**, *22*, 1185.
(28) Chuang, T. J.; Brundle, C. R.; Rice, D. W. *Surf. Sci.* **1976**, *59*, 413.

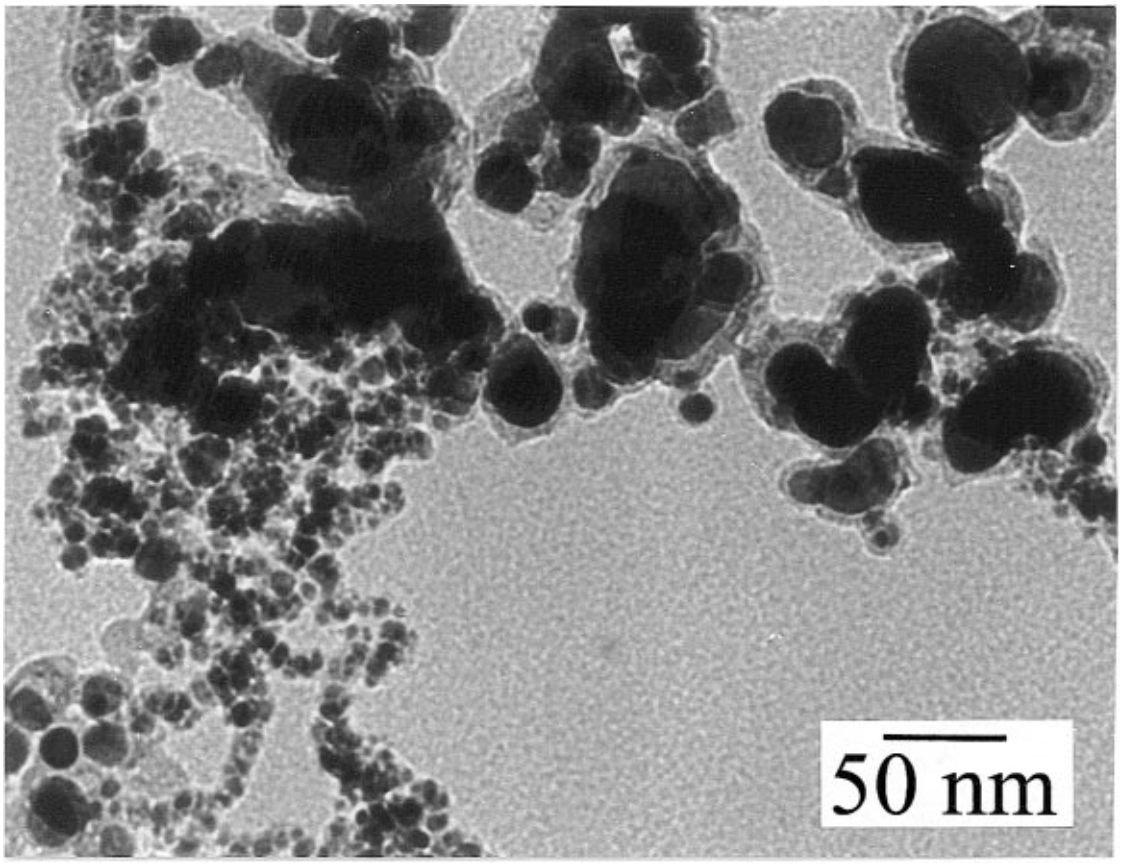

Figure 6. 6. TEM micrography of CCo.

are dissolved during acid washing and are only partially covered with carbon.

3. The Co surface concentration in wCCo is lower than that in CCo. This difference is probably at the origin of the lower catalytic activity of wCCo + AN compared with that of CCo + AN (Figures 2 and 3).

4. The oxygen surface concentrations reported in Table 1 for CCo and wCCo are quite large. Uncoated Zn and Co oxides account for part of it in CCo. However, after their dissolution, the O surface concentration in wCCo still remains large. Thus, the soot produced in the arc discharge contains several oxidized surface groups. This is quite common among carbon blacks. As expected, their concentration decreases by thermal decomposition after pyrolysis at 1000 °C in Ar + AN.[29]

5. The nitrogen surface concentrations are low in CCo and wCCo compared with that of the activated materials. Nitrogen was not introduced on purpose in the electric arc generation of CCo which occurred under low helium gas pressure (125 Torr). It was most probably introduced in the reactor as nitrogen gas adsorbed on the mixture of Co_3O_4, graphite powder, and dextran used to pack the drilled graphite rod of the carbon arc process. The increase in N surface concentrations after activation results from the pyrolysis at 1000 °C of CH_3CN and the accumulation of pyrolyzed C- and N-containing material on the precursors. As an example, exposure of 1 g of carbon black (XC-72R from Cabot) to Ar + AN at 1000 °C caused a 66% weight increase to occur. While the pyrolysis of acetonitrile is at the origin of the catalyst activation and also of the growth of nanotubes seen by TEM (see next section), the accumulation of new material on the surface is also responsible for the decrease in the Co surface concentrations detected by XPS (Table 1).

6. After activation, the N1s XPS spectrum (Figure 5) shows two peaks while only one was observed in the catalyst precursor. The same N1s spectra of CCo + AN and wCCo + AN are identical. The same two N species were also produced by the high-temperature fragmentation of Co or Fe phthalocyanines and porphyrins adsorbed on carbon black.[11,30−32] These pyrolyzed materials are also catalysts for the electroreduction of O_2. The higher energy peak is not necessarily associated with the catalytic site because it is also seen when XC-72R is heat-treated in Ar + AN. This material is not active for the reduction of oxygen in acidic medium.[17]

Recently, the various nitrogen binding energies in N-containing calcinated carbonaceous materials have been estimated theoretically.[33] It was demonstrated that the N1s core level peak may exhibit up to three different components depending upon the heat-treatment temperature. At temperatures below 800 °C, only two components were observed. They were assigned to pyridinic type N atoms (398.6 eV), which contribute to the π system with one p electron and to pyrrolic type N atoms (400.3 eV) contributing two p electrons to the π

(29) Bansal, R. C.; Donnet, J. B. *Carbon Black*, 2nd ed.; Donnet, J. B., Bansal, R. C., Wang, M. J., Eds.; Marcel Dekker, Inc.: New York, 1993; p 175.

(30) Savy, M.; Coowar, F.; Riga, J.; Verbist, J. J.; Bronoël, G.; Besse, S. *J. Appl. Electrochem.* **1990**, *20*, 260.

(31) Widelöv, A.; Larsson, R. *Electrochim. Acta* **1992**, *37*, 187.

(32) Biloul, A.; Coowar, F.; Contamin, O.; Scarbeck, G.; Savy, M.; van den Ham, D.; Riga, J.; Verbist, J. J. *J. Electroanal. Chem.* **1992**, *328*, 219.

(33) Casanovas, J.; Ricart, J. M.; Rubio, J.; Illas, F.; Jiménez-Mateos, J. M. *J. Am. Chem. Soc.* **1996**, *118*, 8701.

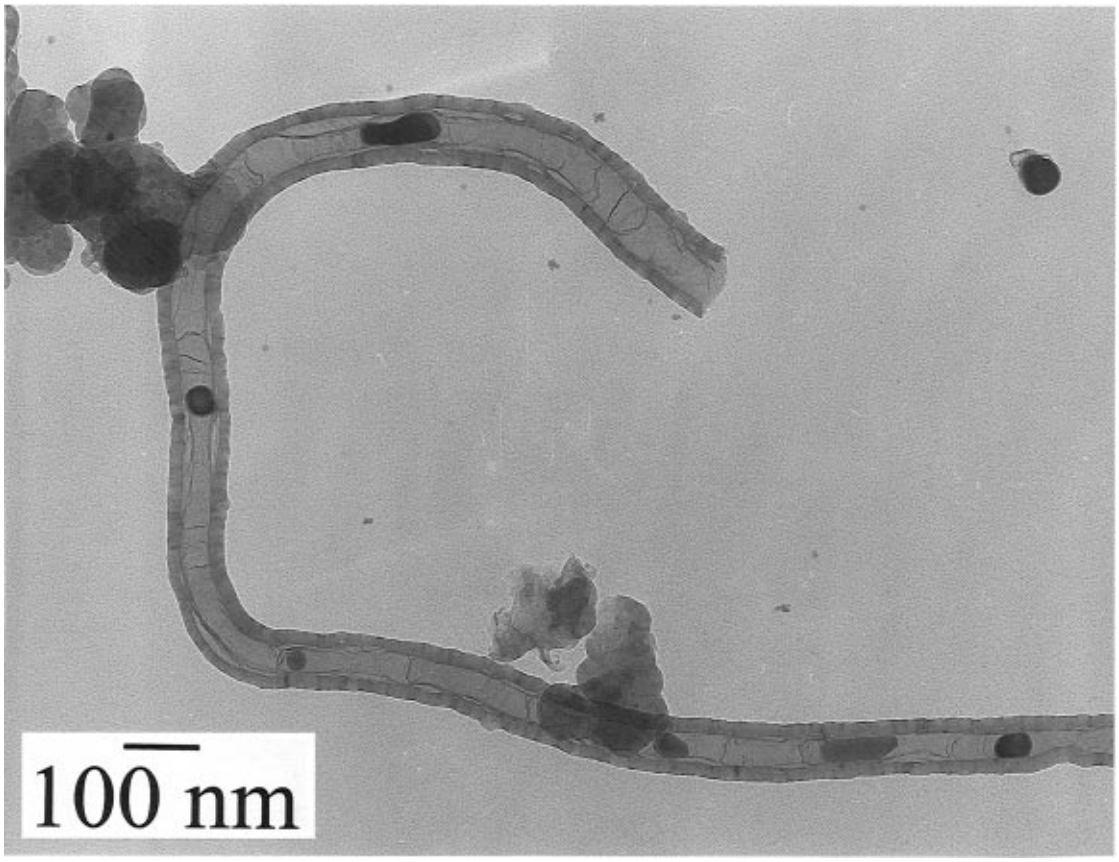

Figure 7. 7. TEM micrography of a nanotubule in CCo + AN.

system. A third component at higher binding energies (401−403 eV) develops at higher temperatures. It corresponds to highly coordinated N atoms substituting some inner C atoms of the graphene layer. It is obvious from Figure 5 that pyridinic type (398.9 eV) and highly coordinated N atoms (401.2 eV) are present in CCo + AN (and wCCo + AN) and that the carbon-based structures observed by TEM (see below) are probably N-doped.

7. The $Co2p_{3/2}$ XPS spectrum of wCCo + AN, presented in Figure 4, is drastically different from that of wCCo, the inactive precursor. It shows a broad maximum at 780 eV, which is a binding energy corresponding to Co^{II}.[27] A similar spectrum is obtained for CCo + AN. The catalytic material may still contain some buried metallic Co, but its surface or the region where the catalytic sites are situated is characterized by oxidized Co. This is in agreement with what was found for PVF adsorbed on carbon black. After pyrolysis at 1000 °C of the latter material in Ar + AN, oxidized Fe was also observed by XPS.[17]

TEM Results. Figure 6 is a micrography of CCo. It shows that the collected soot is composed of carbon-coated clusters of various sizes. A similar picture is obtained for wCCo. Figures 7 and 8 are micrographies of CCo + AN and wCCo + AN, respectively. Besides containing soot particles, the materials also show large, thick-walled nanotubes that may contain Co particles. The coiled nanotubes depicted in Figure 8 are particularly spectacular. Co particles do not seem to be present in the graphitic coils shown in that picture, but they are present in other nanotubes of the same material. Nanotubes are absent from the unactivated materials (CCo and wCCo). They are therefore a result of the pyrolysis step. During this step at 1000 °C in an Ar + AN ambient, supplementary carbon (and nitrogen) is available for the growth of these nanotubes.

The growth of graphitic carbon nanofibers during the decomposition of hydrocarbons in the presence of either supported or unsupported metals has been widely studied.[34−40] Cu, Ni, Fe, and Co particles supported on graphite showed a remarkable activity in decomposing a gas such as acetylene to form filaments.[39,41] The structure of the filaments was different on the various metals. Hollow structures, as in the present work, were formed on the surface of Co and Fe particles, while irregular carbon fibers were deposited on Cu and Ni. Very long tubes (up to 50−60 μm) were obtained by the decomposition of acetylene on graphite-supported Co and even Co oxides.[39]

The formation of graphite nanofibers has been explained according to the following model:[34,42−44] The metal is saturated by the carbon produced by hydro-

(34) Baker, R. T. K. *Carbon* **1989**, *27*, 315.
(35) Sacco, A. Jr.; Geurts, F. W. A. H.; Jablonski, G. A.; Lee, S.; Gately, R. A. *J. Catal.* **1989**, *119*, 322.
(36) Jablonski, G. A.; Geurts, F. W.; Sacco, A. Jr. *Carbon* **1992**, *30*, 87.
(37) Rodriguez, N. M. *J. Mater. Res.* **1993**, *8*, 3233.
(38) Nolan, P. E.; Lynch, D. C. *Carbon* **1994**, *32*, 477.
(39) Ivanov, V.; Fonseca, A.; Nagy, J. B.; Lucas, A.; Lambin, P.; Bernaerts, P.; Zhang, X. B. *Carbon* **1995**, *33*, 1727.
(40) Jiao, J.; Nolan, P. E.; Seraphin, S.; Cutler, A. H.; Lynch, D. C. *J. Electrochem. Soc.* **1996**, *143*, 932.
(41) José-Yacamàn, M.; Miki-Yoshida, M.; Rendon, L.; Santiesteban, J. G. *Appl. Phys. Lett.* **1993**, 62, 657.
(42) Koch, A. J. H. M.; de Bokx, P. K.; Boellaard, E.; Klop, W.; Geus, J. W. *J. Catal.* **1985**, *96*, 468.
(43) Lobo, L. S.; Franco, M. D. *Catal. Today* **1990**, *7*, 247.
(44) Amelinckx, S.; Zhang, X. B.; Bernaerts, D.; Zhang, X. F.; Ivanov, V.; Nagy, J. B. *Science* **1994**, *265*, 635.

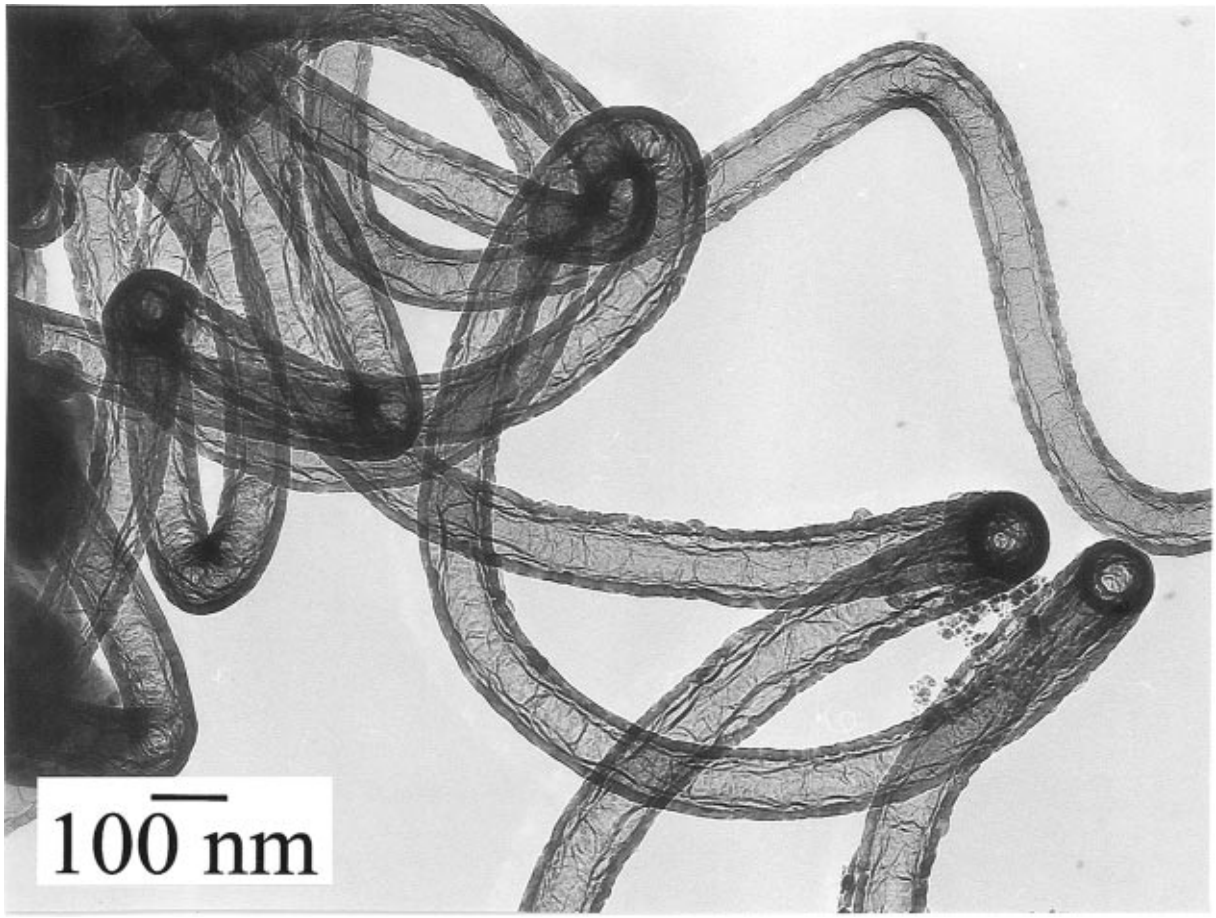

Figure 8. 8. TEM micrography of nanotubules in wCCo + AN.

carbon decomposition, possibly in the form of "active" carbides. The latter then decompose on the surface of the metal to produce graphite fibers. A similar model can be operative in our conditions; at 1000 °C, the carbon surrounding the Co cluster will saturate the metal, reducing to zero in some places the thickness of the irregularly shaped protecting envelope and thus initiating the growth of the tubules.

It is supposed that the metal becomes inactive for nanotube growth when it is introduced into the tubule during the growth process.[39] Such Co particles are seen for instance in Figure 7. The helical growth of nanotubes, as shown in Figure 8, is the result of regular defects introduced in the graphite structure. The introduction of a pentagon−heptagon pair among the hexagonal network has been proposed as the mechanism of coiled nanotube formation.[45]

Nanotubes have been observed after activation of catalytically inactive carbon-coated Co nanocrystallites generated by electric arc discharge. Nanotubes have also been observed after the pyrolysis at 1000 °C in Ar containing AN vapors of catalytically inactive materials such as (i) $Fe(OH)_2/C$[18] and (ii) carbon-coated Fe nanoparticles produced by the pyrolysis of polyvinylferrocene/C in Ar.[17] In all cases, nanotubes and catalytic activity appeared together but they are not necessarily related. In the present conditions, since it is impossible to separate the nanotubes from their support, it is difficult to obtain a definite answer about an eventual participation of nanotubes to the catalytic activity.

Conclusion

It has been demonstrated that it is possible to activate carbon arc generated soot containing carbon-coated metallic cobalt for the reduction of oxygen in polymer electrolyte fuel cells. The activation step involves pyrolysis of the soot at 1000 °C in an Ar + AN ambient. It is therefore confirmed that this is a general procedure to activate any carbon-coated Fe or Co particles as catalysts for O_2 reduction in acidic media. The performance of the catalysts is, however, not equivalent and changes with the nature of the starting material. Important morphological modifications of the soot (appearance of Co-containing nanotubes) and the disappearance of the XPS signal associated with metallic Co (replaced by an XPS signal assigned to oxidized Co) are noticed after the activation step. Only a fraction of the total Co content of the starting material is involved in the activation step. It would be more efficient to produce the catalyst in situ, i.e., during the electric arc discharge. Since it was shown that N and the metal are essential for the production of the catalytic site,[17] one way of doing so would be to replace the oxide filling of the arc electrode by a filling containing Co and N. Alternatively, nitrogen could also be provided as a gas or as a vapor introduced in the reactor during the electrical discharge.

CM960479N

(45) Zhang, X. B.; Zhang, X. F.; Bernaerts, D.; Van Tenderloo, G.; Amelinckx, S.; Van Landuyt, J.; Ivanov, V.; Nagy, J. B.; Lambin, Ph.; Lucas, A. A. *Europhys. Lett.* **1994**, *27*, 141.